Enhancement of the photoelectrochemical properties of Cl-doped ZnO nanowires by tuning their coaxial doping profile

Jiandong Fan, Frank Güell, Cristian Fábrega, Alexey Shavel, Alex Carrete et al.

Citation: Appl. Phys. Lett. **99**, 262102 (2011); doi: 10.1063/1.3673287
View online: http://dx.doi.org/10.1063/1.3673287
View Table of Contents: http://apl.aip.org/resource/1/APPLAB/v99/i26
Published by the American Institute of Physics.

Enhancement of the photoelectrochemical properties of Cl-doped ZnO nanowires by tuning their coaxial doping profile

Jiandong Fan,[1] Frank Güell,[1] Cristian Fábrega,[2] Alexey Shavel,[1] Alex Carrete,[2] Teresa Andreu,[2] Joan Ramón Morante,[1,2] and Andreu Cabot[1,2,a)]
[1]*Departament Electronica, Universitat de Barcelona, Barcelona 08028, Spain*
[2]*Catalonia Institute for Energy Research, IREC, Sant Adria del Besos, Barcelona 08930, Spain*

(Received 4 September 2011; accepted 5 December 2011; published online 27 December 2011)

Arrays of vertically aligned ZnO:Cl/ZnO core-shell nanowires were used to demonstrate that the control of the coaxial doping profile in homojunction nanostructures can improve their surface charge carrier transfer while conserving potentially excellent transport properties. It is experimentally shown that the presence of a ZnO shell enhances the photoelectrochemical properties of ZnO:Cl nanowires up to a factor 5. Likewise, the ZnO shell promotes the visible photoluminescence band in highly conducting ZnO:Cl nanowires. These lines of evidence are associated with the increase of the nanowires' surface depletion layer. © *2011 American Institute of Physics*. [doi:10.1063/1.3673287]

The potential for combined high efficiency charge carrier transport and surface charge carrier transfer/separation has stimulated interest in semiconductor nanowires (NWs) and nanotubes for an ample range of applications. In particular, ZnO nanowires find multiple technological uses where the optimization of the charge carrier transport and transfer is fundamental: e.g., gas sensing, photovoltaics, photodetectors, photocatalysis, and photoelectrocatalysis. In all these applications, ZnO plays multiple roles: (i) it supports the photo- or catalytically-active species; (ii) it plays a catalytic/photocatalytic role itself; (iii) it collects/separates charge carriers from photo-active or catalytically active sites and species; (iv) it provides the avenues for charge carrier transportation between reaction sites or between the reaction/photogeneration/recombination site and the electrodes. This multiplicity of roles makes very strong demands on material qualities. Independent optimization of the various material qualities required for each role is frequently incompatible with the limited degrees of freedom available in a single material. A particularly important case is the simultaneous maximization of charge carrier transfer and transport. While NWs already provide favorable geometry, a promotion of the ZnO electrical conductivity, usually accomplished by extrinsic doping, is still required in those applications where ZnO has an active electronic role. However, high carrier concentrations reduce the extent of the surface space charge region. The narrowing of the surface depletion layer decreases the volume within the nanowires where the presence of an electric field drives charge separation, thus reducing the efficiency of charge carrier transfer/collection/separation.[1–4]

Compositional graded and core-shell nanostructures are interesting architectures that provide higher levels of control over the material's functional properties.[5] In this direction, ZnO/TiO_2 nanostructures have been shown to enhance photovoltaics efficiency.[6,7] ZnO/Al_2O_3 nanostructures provide excellent surface passivation, promoting radiative recombination.[8] Shells of lower band gap materials can extend the NW's core optical absorption to the visible part of the spectrum, thus promoting charge carrier photogeneration.[9] Nevertheless, the use of coaxial heterojunctions has the challenge of the lattice mismatch, which generally introduces a significant density of interface defects that can decrease the optoelectronic properties of the formed heterostructure.

In this work, we show that adjusting the surface doping level in ZnO:Cl nanowires promotes their surface charge transfer and photoelectrochemical properties without influencing their core's charge carrier concentration. Our goal is to show that it is feasible to produce coaxial homojuntion nanowires with controlled surface depletion layers but conserving their optical properties and their high bulk electrical conductivity. Such control of the surface depletion regions in coaxial homojunction nanowires opens new perspective for the production of more efficient photoelectrochemical, photovoltaic, or photocatalytic devices.

Coaxial ZnO:Cl/ZnO nanowires were grown by a simple electrodeposition two-step process. First, arrays of vertically aligned and single crystal ZnO:Cl NWs were produced by electrodeposition from a solution containing $Zn(NO_3)_2{\cdot}4H_2O$ and NH_4Cl, as previously reported.[10] The carrier density of these NWs was previously estimated to be close to $10^{19}\,cm^{-3}$.[10] To obtain coaxial ZnO:Cl/ZnO homojunction, the initial ZnO:Cl NWs were thoroughly washed in water and subsequently subjected to one or more additional electrodeposition growth steps in the absence of NH_4Cl. The thickness of the ZnO shell was controlled by the electrodeposition time and/or the number of additional electrodeposition growth steps.

Figure 1 shows scanning electron microscopy (SEM) images of the ZnO:Cl before and after growing a 15 nm ZnO shell. As expected from the epitaxial growth of the ZnO shell, at first view, no clear differences between the ZnO:Cl and the ZnO:Cl/ZnO NWs were observed in the SEM images. Importantly, neither branching nor nucleation of additional nanowires or nanoparticles was observed. Statistical measurements of the nanowires dimensions allowed us to determine their ZnO shell thickness (~15 nm) and the shell growth rate in the used electrodeposition conditions (~36 nm/h) (Fig. 1(c)). This value was consistent with x-ray photoelectron spectroscopy

a)Author to whom correspondence should be addressed. Electronic mail: acabot@irec.cat. Tel.: +34625615115. Fax: +34934021148.

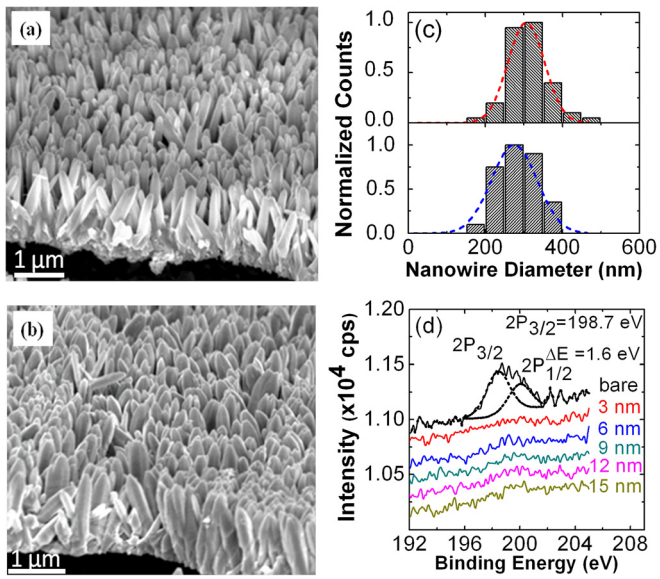

FIG. 1. (Color online) Cross-section SEM images of bare ZnO:Cl nanowires (a) and ZnO:Cl/ZnO homojunction nanowires with a 15 nm shell thickness (b). (c) Histograms of the thickness distribution of the ZnO:Cl/ZnO (up) and the bare ZnO:Cl (down) nanowires. (d) Chlorine region of the XPS spectra of ZnO:Cl and ZnO:Cl/ZnO nanowires with increasingly thicker shell thicknesses as noted in the graph. The fitting of the chlorine 2P band with two peaks, corresponding to $2P_{3/2}$ and $2P_{1/2}$ is also shown.

(XPS) characterization of the evolution of the Cl composition with the shell thickness (Fig. 1(d)). For these measurements, the same sample was subjected to successive ZnO growth steps while an XPS spectrum was obtained in between each step. The Cl concentration was already below the XPS detection limit in ZnO:Cl/ZnO NWs with a shell grown for 5 min, which roughly corresponded to a 3 nm width. The lack of Cl signal from the ZnO:Cl/ZnO samples also pointed towards a highly homogeneous ZnO deposition on the surface of the ZnO:Cl NWs.

Figure 2 shows the UV-vis spectra of ZnO:Cl/ZnO NWs obtained from the exact same initial ZnO:Cl NWs, which underwent 5 successive ZnO growth steps. UV-vis spectra of the ZnO:Cl/ZnO NWs were obtained in between each electrodeposition step. The optical band gap showed a slight red shift with the successive ZnO growth steps. The origin of such a red shift was found on the optical band gap of the original ZnO:Cl NWs, which was slightly blue-shifted respect

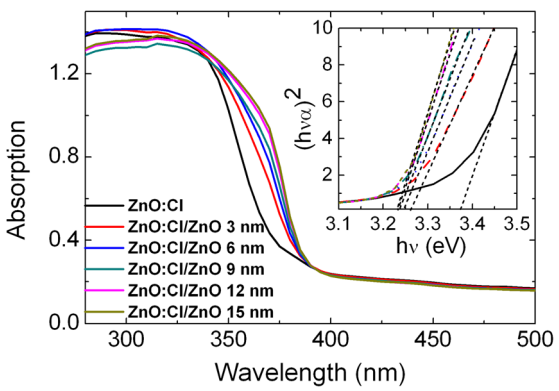

FIG. 2. (Color online) Absorbance spectra of ZnO:Cl nanowires and ZnO:Cl/ZnO homojunction nanowires with increasingly thicker shell thicknesses. The inset shows the dependence of $(\alpha h\nu)^2$ vs. $h\nu$ and the lineal fit used to point the shift of the optical band gap.

to pure ZnO NWs due to the Moss-Burstein effect.[10–13] The growth of a pure ZnO shell on the surface of the ZnO:Cl NWs introduced empty states in the conduction band which allowed the recovery of the electron transitions between the valence band maximum and the conduction band minimum, thus recovering the pure-ZnO optical band gap. The absolute absorbance above the semiconductor band gap did not significantly change with the increase of the ZnO shell thickness. This is consistent with the small increase of the total ZnO volume associated with the growth of the thin ZnO shell.

Figure 3 shows the results from the room-temperature photoluminescence (PL) measurements of ZnO:Cl/ZnO NWs obtained using a HeCd CW laser (325 nm). PL spectra were measured using the exact same ZnO:Cl NWs which were subjected to 5 successive electrodeposition steps to grow an increasingly thicker ZnO shell. Quite unexpectedly, the intensity of the PL peak corresponding to the band-to-band transition decreased slightly with the growth of the pure ZnO shell. At the same time, an enhancement of the PL broad band in the visible part of the spectrum was observed. While the area of the band-to-band PL peak was reduced by a factor 1.7, the visible emission increased almost a factor 4 from the bare ZnO:Cl NWs to the ZnO:Cl/ZnO NWs, which has the thickest ZnO shell tested here (inset in Fig. 3). The enhancement of the visible band with the ZnO shell could be originated by a higher density of impurities introduced by a more-defective ZnO shell when compared with the ZnO:Cl core. However, no evidence was found to support this hypothesis.

The visible band emission in ZnO is associated with impurity levels within the ZnO structure.[14,15] The variety of possible transition and the diversity of ZnO preparation and sintering procedures employed did not allow a consensus on the exact origin of the energy levels contributing to these transitions. In ZnO NWs, the intensity of the visible band has been previously correlated with the materials surface-to-bulk ratio.[16] Such correlation pointed towards an important role of the surface in the associated radiative recombination processes.[14,16–19] Again, there is no agreement on the origin of such a surface enhancement of the visible band in NWs. It

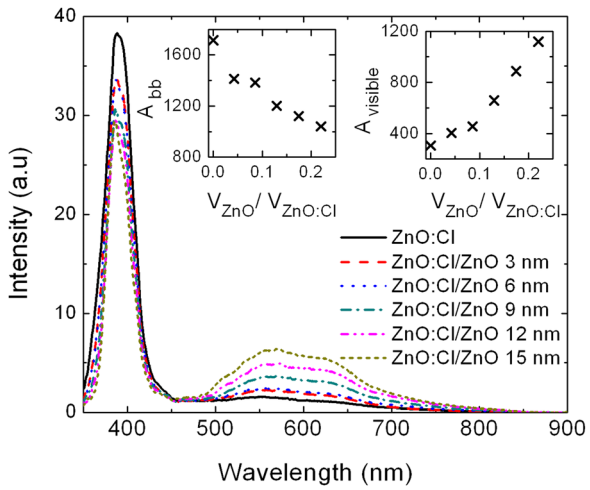

FIG. 3. (Color online) Room temperature photoluminescence spectra of ZnO:Cl nanowires and ZnO:Cl/ZnO homojunction nanowires with increasingly thicker shell thicknesses obtained using 325 nm excitation wavelength. Insets show the evolution of the photoluminescence peak area corresponding to the band-to-band transition and to the visible emission, as noted.

could be related with a higher surface density of the contributing states, their surface activation by the hole accumulation at the surface depletion, or the promotion of slower recombination processes related with the charge separation occurring in the built-in electric field layer.[8,14,20–26]

In ambient conditions, the ZnO NWs surface is covered by ionized oxygen species and hydroxyl groups that trap conduction electrons, causing an upward bending of the ZnO energy bands at the surface. While highly doped ZnO screens the surface charge within a very thin surface layer, much thicker depletion regions characterize undoped semiconductors. Considering a typical barrier height of 0.55 eV,[27] the width of the calculated depletion layer increases from 7 to 230 nm when reducing the carrier concentration from $10^{19}\,cm^{-3}$ to $10^{16}\,cm^{-3}$.[27–29] In this scenario, the growth of an undoped ZnO shell on the surface of ZnO:Cl NWs offers an effective way to adjust the depletion region without modifying the NW's bulk conductivity (Fig. 4(d)).

The excellent correlation existing between the increase of the visible PL band intensity and the growth of the surface depletion layer when increasing the ZnO shell thickness points towards a direct role of the surface band bending in the promotion of the visible PL. This is consistent with previous studies.[16,20] The parallel reduction of the interband PL intensity may be associated with a shell screening of both the incident UV photons and of those emitted by the NWs core.

The increase of the depletion layer by the presence of the ZnO shell also augments the volume for charge photogeneration within the nanowires where the presence of an electric field drives charge separation.[30] Charge carriers photogenerated in the bulk ZnO need to diffuse to reach the depletion layer where an electric field can drive holes to the surface. However, in bulk ZnO, the holes, the minority carriers, have short diffusion length as they rapidly recombine with electrons, the majority carriers, inside the bulk. In contrast, when photogeneration takes place in the depletion layer, carriers are rapidly separated and swept in opposite directions by the built-in electric field.

The promotion of the charge carrier separation and transfer by the presence of a ZnO shell was verified by the characterization of the NWs photoelectrochemical (PEC) properties in a standard three-electrode cell using UV excitation from an HgXe lamp (Fig. 4(c)). In Fig. 4(a), the photocurrent generated by the ZnO:Cl/ZnO NWs is shown. Again, the same NWs were measured in between successive ZnO electrodeposition steps to avoid any effect of the NWs geometry, density, or compositional differences from batch to batch. The photocurrent measured from the ZnO:Cl/ZnO NWs was clearly promoted by the presence of the ZnO shell. Up to a 5-fold increase of the photocurrent was obtained with a 12 nm thick ZnO shell, from 0.6 mA/cm^2 to 3.1 mA/cm^2. Both the correlation of the PEC enhancement with the ZnO shell thickness and the apparent photocurrent saturation for shells thicker than 12 nm were systematically obtained (Fig. 4(b)). The relatively low photocurrent saturation thickness is most probably related to the non-intrinsic character of the ZnO shell. While no extrinsic doping was intentionally introduced, it is well known that electrodeposited ZnO contain significant densities of n-type impurities, which translate into carrier concentrations in the range of 10^{17}.[10] At the same time, a considerable number of charge carriers are transferred from the ZnO:Cl core to the ZnO shell when forming the homojunction. Both effects may explain the relatively low saturation thicknesses obtained.

In summary, the control of the doping profile in ZnO:Cl/ZnO NWs allowed adjustment of the thickness of the depletion layer and the volume within the NWs with a built-in electric field. Such homojunction nanowires promote charge separation and transfer to the surface as evidenced by an enhancement of the surface-related PL band and the

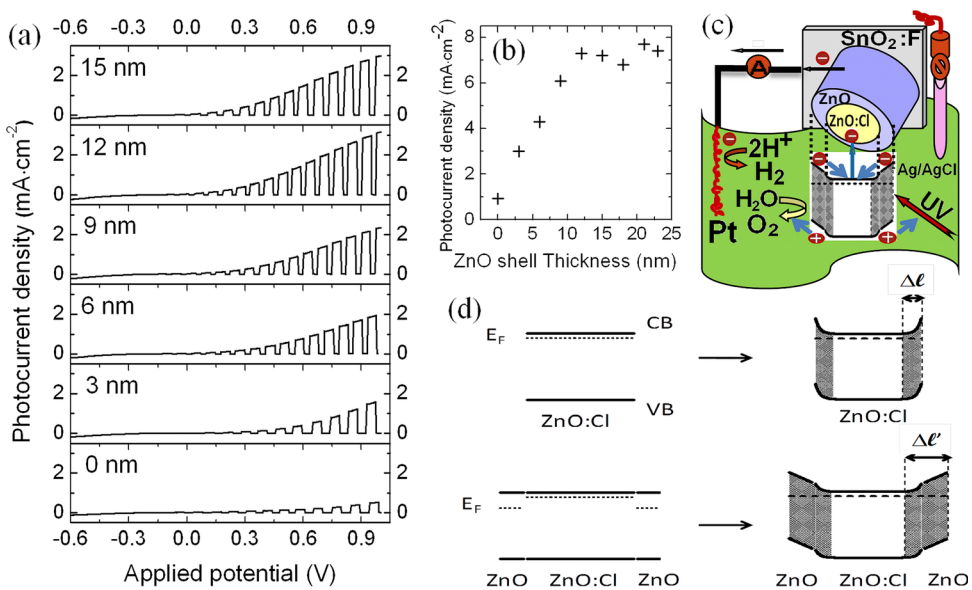

FIG. 4. (Color online) (a) Photocurrent density vs. applied potential (V vs. Ag/AgCl) for ZnO:Cl nanowires and ZnO:Cl/ZnO homojunction nanowires with increasingly thicker shell, measured under chopped UV illumination (100 mW/cm^2) in 0.1 M Na_2SO_4 aqueous solution. (b) Photocurrent as a function of the shell thickness for a second set of ZnO:Cl and ZnO:Cl/ZnO nanowires. (c) Schematic illustration of the photoelectrochemical reaction taking place at the ZnO:Cl/ZnO nanowire surface. Photogenerated carriers are separated at the depletion region. Holes are driven to the surface where the water oxidation reaction takes place. Electrons are swept to the nanowire core and funnelled inside there towards the platinum electrode where the reduction reaction takes place. (d) Band diagrams of the ZnO:Cl and ZnO:Cl/ZnO nanowires illustrating the increase of the surface depletion region with the growth of the ZnO shell.

improvement of the PEC properties of the material. We believe such core-shell homojunction nanowires are good candidates to improve the efficiency of photoelectrochemical, photocatalytic and photovoltaic devices.

This work was supported by the Spanish MICINN Projects MAT2008-05779, MAT2008-03400-E/MAT, MAT2010-15138, MAT2010-21510, CSD2009-00050, and ENE2008-03277-E/CON. J.F. and T.A. thank the FI-DGR and BP grants from the Agència de Gestió d'Ajuts Universitaris i de Recerca (AGAUR) from the Catalan Government. A.C. thanks financial support through the Ramón y Cajal program. We also thank Dr. Robin Rycroft for his kind help to polish the English.

[1]M. Ono, K. Fujii, T. Ito, Y. Iwaki, A. Hirako, T. Yao, and K. Ohkawa, J. Chem. Phys. **126**, 054708 (2007).
[2]J. Reichman, Appl. Phys. Lett. **36**, 574 (1980).
[3]W. W. Gartner, Phys. Rev. **116**, 84 (1959).
[4]C.-T. Sah, R. N. Noyce, and W. Shockley, Proc. IRE **45**, 1228 (1957).
[5]C. R. Hall, L. V. Dao, K. Koike, S. Sasa, H. H. Tan, M. Inoue, M. Yano, C. Jagadish, and J. A. Davis, Appl. Phys. Lett. **96**, 193117 (2010).
[6]L. E. Greene, M. Law, B. D. Yuhas, and P. Yang, J. Phys. Chem. C **111**, 18451 (2007).
[7]M. Law, L. E. Greene, A. Radenovic, T. Kuykendall, J. Liphardt, and P. Yang, J. Phys. Chem. B **110**, 22652 (2006).
[8]J.-P. Richters, T. Voss, D. S. Kim, R. Sholz, and M. Zacharias, Nanotechnology **19**, 305202 (2008).
[9]X. Wang, H. Zhu, Y. Xu, H. Wang, Y. Tao, S. Hark, X. Xiao, and Q. Li, ACS Nano **4**, 3302 (2010).
[10]J. Fan, A. Shavel, R. Zamani, C. Fábrega, J. Rousset, S. Haller, F. Güell, A. Carrete, T. Andreu, J. Arbiol, J. R. Morante, and A. Cabot, Acta Mater. **59**, 6790 (2011).
[11]E. Burstein, Phys. Rev. **93**, 632 (1954).
[12]T. S. Moss, Proc. Phys. Soc. London, Sec. B **67**, 775 (1954).
[13]J. G. Lu, S. Fujita, T. Kawaharamura, H. Nishinaka, Y. Kamada, T. Ohshima, Z. Z. Ye, Y. J. Zeng, Y. Z. Zhang, L. P. Zhu, H. P. He, and H. Zhao, J. Appl. Phys. **101**, 083705 (2007).
[14]A. B. Djurišić, A. M. C. Ng, and X. Y. Chen, Prog. Quantum Electron. **34**, 191 (2010).
[15]C. V. Manzano, D. Alegre, O. Caballero-Calero, B. Alén, and M. S. Martín-González, J. Appl. Phys. **110**, 043538 (2011).
[16]I. Shalish, H. Temkin, and V. Narayanamurti, Phys. Rev. B **69**, 245401 (2004).
[17]J. D. Prades, A. Cirera, J. R. Morante, and A. Cornet, Thin Solid Films **515**, 8670 (2007).
[18]X. Gu, K. Huo, G. Qian, J. Fu, and P. K. Chu, Appl. Phys. Lett. **93**, 203117 (2008).
[19]P.-C. Chang, C.-J. Chien, D. Stichtenoth, C. Ronning, and J. G. Lu, Appl. Phys. Lett. **90**, 113101 (2007).
[20]S. Shi, J. Xu, X. Zhang, and L. Li, J. Appl. Phys. **109**, 103508 (2011).
[21]A. van Dijken, E. A. Meulenkamp, D. Vanmaekelbergh, and A. Meijerink, J. Phys. Chem. B **104**, 1715 (2000).
[22]A. van Dijken, E. A. Meulenkamp, D. Vanmaekelbergh, and A. Meijerink, J. Phys. Chem. B **104**, 4355 (2000).
[23]K. Vanheusden, W. L. Warren, C. H. Seager, D. R. Tallant, J. A. Voigt, and B. E. Gnade, J. Appl. Phys. **79**, 7983 (1996).
[24]J. D. Ye, S. L. Gu, F. Qin, S. M. Zhu, S. M. Liu, X. Zhou, W. Liu, L. Q. Hu, R. Zhang, Y. Shi, and Y. D. Zheng, Appl. Phys. A **81**, 759 (2005).
[25]R. L. House, B. P. Mehl, J. R. Kirschbrown, S. C. barnes, and J. M. Papanikolas, J. Phys. Chem. C **115**, 10806 (2011).
[26]Z.-M. Liao, H.-Z. Zhang, Y.-B. Zhou, J. Xu, J.-M. Zhang, and D.-P. Yu, Phys. Lett. A **372**, 4505 (2008).
[27]Z.-M. Liao, K.-J. Liu, J.-M. Zhang, J. Xu, and D.-P. Yu, Phys. Lett. A **367**, 207 (2007).
[28]J. D. Prades, F. Hernandez-Ramirez, R. Jimenez-Diaz, M. Manzanares, T. Andreu, A. Cirera, A. Romano-Rodriguez, and J. R. Morante, Nanotechnology **19**, 465501 (2008).
[29]I. Mora-Seró, F. Fabregat-Santiago, B. Denier, J. Bisquert, R. Tena-Zaera, J. Elias, and C. Lévy-Clément, Appl. Phys. Lett. **89**, 203117 (2006).
[30]L. L. Yang, Q. X. Zhang, M. Q. Israr, J. R. Sadaf, M. Willander, G. Pozina, and J. H. Yang, J. Appl. Phys. **108**, 103513 (2010).